J Neural Transm (2017) 124:685–694
DOI 10.1007/s00702-017-1718-7



# Alzheimer's senile plaque as shown by microcryodissection, a new technique for dissociating tissue structures

**Manon Thierry[1,2] · Serge Marty[1] · Susana Boluda[1,2] · Charles Duyckaerts[1,2]**

Received: 18 October 2016 / Accepted: 27 March 2017 / Published online: 6 April 2017


**Abstract** Extracellular accumulation of Aβ peptides and intracellular aggregation of hyperphosphorylated tau proteins are the two hallmark lesions of Alzheimer disease (AD). The senile plaque is made of a core of extracellular Aβ surrounded by phospho-tau positive neurites. It includes multiple components such as axons, synapses, glial fibers and microglia. To visualize the relationships of those elements, an original technique was developed, based on the dilation of interstitial water during freezing. Samples of neocortex, hippocampus and striatum were taken from formalin-fixed brains (one control case; three cases with severe Alzheimer disease). The samples were subjected to various numbers of freezing/thawing cycles (from 0 to 320) with an automated system we devised. The samples were embedded in paraffin, cut and stained with haematoxylin-eosin or immunostained against Aβ, phospho-tau, and antigens enriched in axons, synapses, macrophages or astrocytes. Microcryodissection induced the dissociation of tissue components, especially in the grey matter where the neuropil formed an oriented "mesh". The size of the empty spaces separating the fiber bundles and cells increased with the number of cycles. The amyloid core of the senile plaque separated from its neuritic crown at around 300 freezing/thawing cycles. The dissected core remained associated with macrophages containing Aβ in their cytoplasm. Phospho-tau positive axons were distinctly seen projecting from the neuritic crown to the isolated amyloid core, where they ended in large synapses. The microcryodissection showed astrocytic processes stuck directly to the core. The original method we developed—microcryodissection—helped understanding how histological components were assembled in the tissue.

**Keywords** Microcryodissection · Klingler's method · Senile plaque · Alzheimer

## Introduction

Alzheimer's disease (AD) is characterized by extracellular accumulation of β-amyloid peptides (Aβ) and intraneuronal aggregation of hyperphosphorylated tau proteins (HP-tau). Tau and Aβ accumulation occurs in the senile plaque, a complex lesion that is one of the hallmarks of AD pathology. The senile plaque is made of an Aβ deposit, eventually concentrated in an amyloid core, surrounded by a phospho-tau positive neuritic crown (Duyckaerts et al. 2009). Astrocytic processes, axons, synapses, macrophages and possibly dendrites are also involved in the complex structure of the senile plaque. The relationships of those components are difficult to disentangle. In this study, we developed a new and original technique to dissociate the senile plaque (and more generally, histological structures). The method, microcryodissection, is based on the dilation of interstitial water obtained by freezing the tissue [inspired by Klingler's method (Ludwig and Klingler 1956)]. Water is excluded from the lipid-rich membranes and accumulates within the space separating them. The dilation of water, during the freezing stage, is followed by thawing during which water

**Electronic supplementary material** The online version of this article (doi:10.1007/s00702-017-1718-7) contains supplementary material, which is available to authorized users.

✉ Manon Thierry
manon.thierry@icm-institute.org

[1] Alzheimer's and Prion Diseases Team, Institut du Cerveau et de la Moelle Epinière, CNRS UMR 7225, INSERM 1127, UPMC UM75, Paris, France

[2] Laboratoire de Neuropathologie Raymond ESCOUROLLE, Paris, France

accumulates in the holes left by the contraction of water when switching from solid to liquid state. Repeating the cycles gradually dissects the hydrophobic, lipid rich structures, from the water-containing interstitium (Fig. 1).

## Materials and methods

### Cases

Four brains were investigated. They had been collected in a brain donation project and stored in the national brain bank NeuroCEB (bioresource research impact factor number BRIF BB-0033-00011). Case 1 (control) was a 92 years old woman with no Aβ pathology and only a few tau positive neurites and neurofibrillary tangles in the entorhinal cortex and anterior hippocampus (Braak neurofibrillary stage III, Thal amyloid phase 0 (Braak and Braak 1991; Thal et al. 2002). Cases 2, 3 and 4 were a woman and two men of 73, 62 and 68 years of age, respectively, with severe AD lesions (Braak VI, Thal 5).

### Preparation of the human samples

The neocortex (area 22), hippocampus and striatum were resampled from brains which had been stored in buffered formalin 10% (formaldehyde 4%) for 1, 2, 3 or 5 years. The samples, with an area of approximately 2 $cm^2$, and a thickness of 3 mm, were submitted to freezing/thawing cycles induced by an automated system developed in this laboratory (supplementary Fig. S1). The device was made of a Peltier thermoelectric cooler (TEC1-12706, Hebei I.T., Shanghai, China) powered by a 12 V, 5 A supply and cooled by a heatsink with a fan taken from a used power supply of a computer. The fan was powered through a USB plug. The circuit was interrupted by a relay connected with a computer (USB one relay, KMtronic Ltd, Bulgaria). A batch file was programmed to ensure a cycle of 700 s on (to freeze the sample) and 300 s off (to thaw it and to cool the device). One sample of neocortex (case 2) was sectioned into nine subsamples. The subsamples were subjected to an increasing number of freezing/thawing cycles ($n = 0, 1, 5, 10, 20, 40, 80, 160, 320$). After establishing that the best results were obtained with 320 freezing/thawing cycles (Fig. 2), all the other samples (cases 1, 3 and 4) were subjected to at least 300 cycles, i.e. alternative freezing and thawing for 5000 min or 3 days and a half. The microcryodissected samples were embedded in paraffin. Histologic sections were cut from the block at a thickness of 3 µm.

### Preparation of the mouse samples

Three PS1 mice (used as controls of APPxPS1 mice), devoid of plaques were used to test the possibility of a

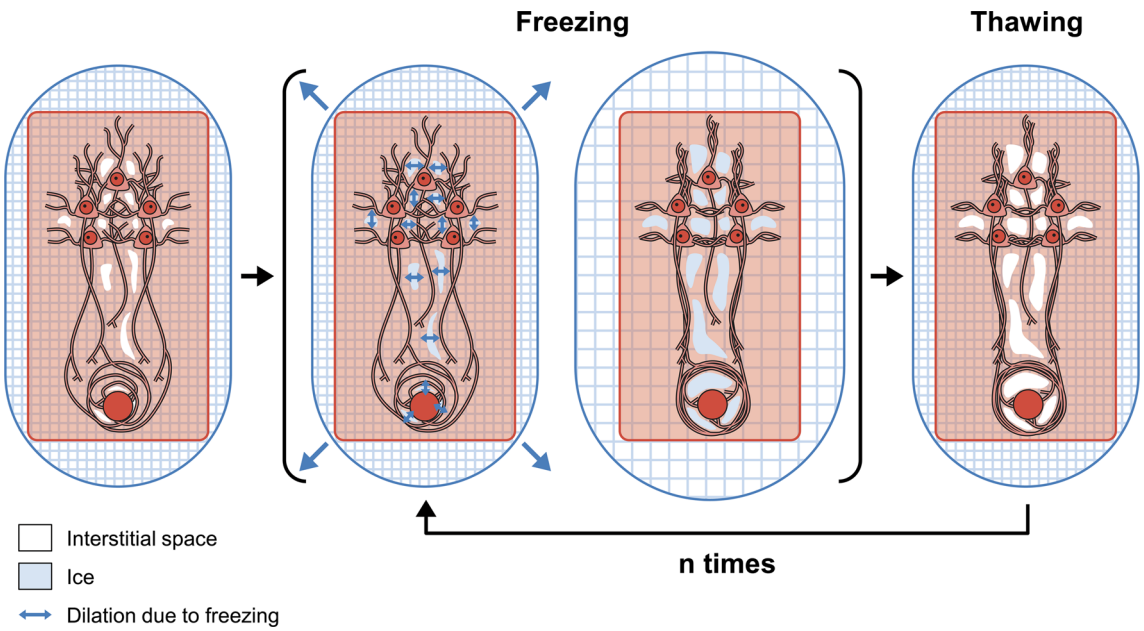


**Fig. 1** Diagram representing the principle of microcryodissection. The *blue grid* represents water in contact with the brain sample (*red rectangle*). Water does not penetrate the lipid-rich membranes, and fills the interstitium. The dilation of water caused by freezing (*blue arrows*) induces the expansion of interstitial spaces (*ice in blue*) within the tissue components. During thawing, more water accumulate in the enlarged interstitial spaces. Water is represented in *white*. Successive freezing/thawing cycles amplify the process (≥300 cycles in this study). Five neurons and a senile plaque containing an amyloid core (*red circle*) surrounded by a neuritic crown made of axons are represented within the brain section, surrounded by an interstitial space

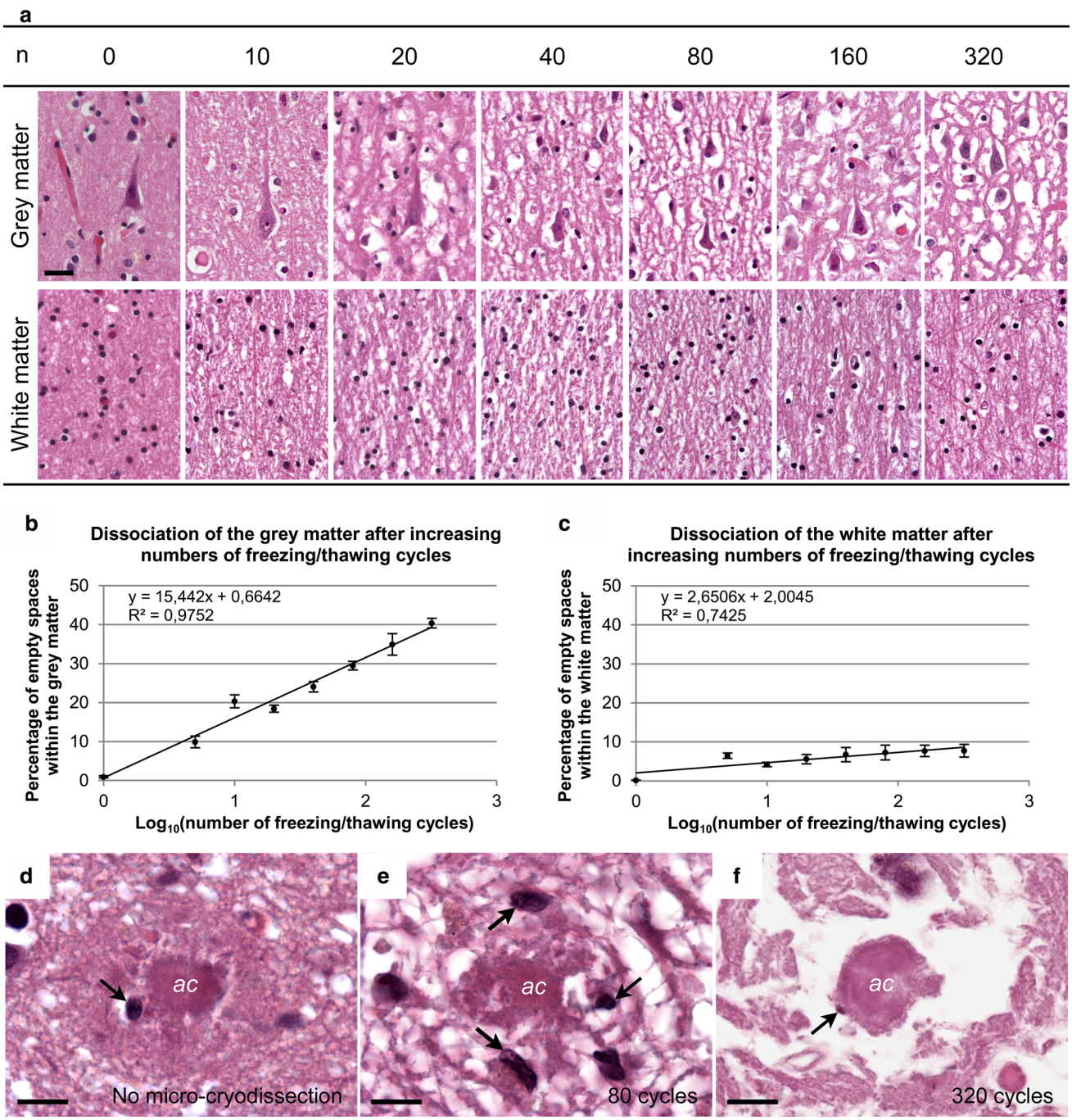


**Fig. 2** Effects of microcryodissection at various number of freezing/thawing cycles. **a** Human brain. Haematoxylin–eosin stain. *Scale bar* 20 µm. Aspects of the neocortex (*upper row*) or white matter (*lower row*) after *n* freezing/thawing cycles (*n* from 0 to 320). The effects of microcryodissection in the subcortical white matter were limited. In the neuropil, fibers were best dissociated after 80 cycles. Beyond that value, fibers tended to aggregate into oriented fascicles that formed an organized mesh. **b** and **c** Means of the proportion of empty spaces within the grey matter (**b**) or within the white matter (**c**), as a function of $\log_{10}$ (*n*), *n* being the number of freezing/thawing cycles. The means are obtained from six microscopic fields, observed at a ×10 magnification. The equation of the linear regression is given, as well as the coefficient of determination. **d**–**f** Human brain. Haematoxylin–eosin stain. *Scale bar* 8 µm. Senile plaques observed without microcryodissection (**d**), after 80 cycles (**e**) or after 320 cycles (**f**). The amyloid core (*ac*) of the senile plaque was best dissociated from its neuritic crown after 320 cycles. Macrophages (*arrows*) appeared to be associated with the amyloid core

different reactivity of rodent tissue to cryodissection. Brains were formalin fixed by immersion. Sagittally sectioned hemispheres were subjected to 80 or 320 freezing/thawing cycles. The samples were embedded in paraffin, sectioned at a 3 µm thickness, deparaffinized, and stained with haematoxylin–eosin.

### Immunohistochemistry

Immunohistochemistry (IHC) was performed with the automated Nexes station (Roche Ventana Medical Systems)—except for Aβ IHC which required a longer incubation period, not possible to achieve with the automated system. Deparaffinized and rehydrated sections were pretreated, and then incubated with the primary antibodies (see the supplementary table for details). Primary antibodies directed against phospho-tau (AT8), myelin basic proteins (MBP), synaptophysin, CD68, glial fibrillary acidic protein (GFAP) and ubiquitin were detected with the *ultra*View Universal DAB kit (Ventana Medical Systems), according to the procedure XT ultraView DAB v3 summarized in the supplementary table. The kit includes secondary antibodies (goat anti-mouse IgG, anti-mouse IgM and anti-rabbit) conjugated with horseradish peroxidase polymers. The addition of $H_2O_2$ and DAB leads to the formation of a brown precipitate. For the double labeling with the anti-phospho-tau AT8 and anti-Aβ 6F3D or with anti-MBP and anti-NF, two rounds of immunolabeling, separated by washing and heat denaturation, were performed. During the first round, the first primary antibody was labeled with secondary antibodies coupled with peroxidase that oxidized DAB into a brown precipitate. The sections were then incubated with the second primary antibody, revealed by the *ultra*View Universal Alkaline Phosphatase Red detection kit (Ventana Medical Systems), used according to the XT IHC Double Staining uDAB-uRed v3 procedure summarized in the supplementary table. The kit includes secondary antibodies (goat anti-mouse IgG, anti-mouse IgM and anti-rabbit) conjugated with alkaline phosphatase polymers. The addition of naphthol and Fast Red leads to the formation of a red precipitate. The anti-Aβ 6F3D IHC was performed manually following the steps summarized in the supplementary table, using DAB for detection (ChemMate Dako detection kit). Sections were counterstained with Harris haematoxylin.

### Assessment of the volume change of the sample related to freezing–thawing

Samples were left on graph pictures before and after the series of freezing–thawing cycles. Pictures were taken. The main axes of the samples were manually measured on the pictures.

### Quantification of the increase in empty space caused by microcryodissection

The nine neocortical subsamples of case 2 were subjected to an increasing number of freezing/thawing cycles (see above). The samples were embedded in paraffin, and cut at 3 μm. The deparaffinized and rehydrated sections were stained with haematoxylin–eosin. For each section, 12 pictures were taken in the grey matter ($n$ fields = 6) and in the white matter ($n$ fields = 6). The expansion of the empty spaces was assessed using Image J. Pictures were converted into 8-bit images and binarized using the black and white mode, after setting the threshold at a level where the whole picture appeared white except the empty spaces that were shown in black. The proportion of black (empty spaces) over white pixels (all other structures) was then calculated. Blood vessels were excluded from the analysis, to avoid bias due to the presence of Virchow–Robin spaces. The superficial layers (I and II) of the cortex were also excluded from the quantification, since a spongiosis likely due to Alzheimer's disease could be observed in the unprocessed sample. We tested several types of functions with the aim of fitting the observation points to a theoretical curve. The goodness of fit was evaluated by the coefficient of determination $R^2$.

### Electron microscopy

Three samples from the frontal cortex were removed from a formalin-fixed brain (case 3). The samples were submitted to the 80 or 320 freezing/thawing cycles and compared to a sample that was commonly processed. Each sample was sliced into 200 μm sections using a vibratome (Leica, Vienna, Austria). For each condition, small areas of $1 \times 1 \times 0.2$ mm$^3$ were taken from the grey matter, where the plaques were more abundant, and collected in Phosphate Buffered Saline (PBS). After several washes in Phosphate Buffer (PB), they were transferred into a 1% osmium solution for 1 h. After several washes in water, they were stained "en bloc" with a 5% uranyl acetate solution for 30 min. After several washes, the samples were dehydrated in graded ethanol followed by acetone. They were incubated in 50% acetone-50% epon overnight, followed by epon for 2 h, before being embedded. Sections were cut using a Leica EM UC7 (Leica, Vienna, Austria). For light microscopy, 0.5 μm-thick semi-thin sections were collected on glass slides. For electron microscopy, 70 nm-thick ultrathin sections were collected on copper grids. Ultrathin sections were analyzed with a Hitachi HT 7700 electron microscope (Elexience, Verrieres le Buisson, France) and a $2048 \times 2048$ AMT XR41-B CCD camera (Elexience).

## Results

### Change in the volume of the sample and of the empty spaces present in the section

There was no macroscopic change in the macroscopic volume of the samples whatever the number of freezing/

thawing cycles. The empty spaces contained in the section increased with the number of cycles. Curve fitting approximation indicated that the percentage of space occupied by the empty spaces in the grey matter increased with the number of cycles according to the following equation: $E = a \times \log_{10}(n) + b$ ($r = 0.99$; coefficient of determination $R^2 = 0.9752$); $E$ being the empty areas found in the section, expressed as a percentage, and $n$ being the number of cycles. The constant $a$ is 15.442 and the constant $b$ is close to zero (0.664). For the control (no freezing), the $Y$ value for $n = 0$ was taken as zero to avoid the singularity of log(0). In practice, the equation means that the area occupied by empty spaces is increased twofold from 10 to 100 cycles and threefold from 10 to 1000. Similar results were observed in the white matter, with $a = 2.651$ and $b = 2.005$. ($r = 0.86$; coefficient of determination $R^2 = 0.7425$). Comparison of the slopes for the grey (15.442) and the white (2.651) matter indicates that the expansion is nearly six times larger in the former (Fig. 2).

### Effects of microcryodissection on the tissue components

As expected from the previous paragraph, dissociation of the tissue was particularly marked in the grey matter. Dissection of the axons was limited in the white matter, but sufficient to show the orientation of the fiber fascicles. The dissection of the fibers of the grey matter was best at 80 freezing/thawing cycles, but more homogeneous at 320 cycles where fibers gathered into an oriented "mesh". Results were similar in the mouse brain (supplementary Fig. S2). In the human, the amyloid core of the senile plaque separated best from the crown at 320 cycles—a number of cycles which was thus chosen to study the senile plaque (Fig. 2). The extent of the dissection was inversely proportional to the abundance of myelinated fibers. In the lenticular nucleus, for instance, the grey matter of the putamen (Pu) was more dissociated than the pallidum (Pa) enriched in myelinated fibers. Neurons, glial cells and vessels were well-preserved and often separated from the other components of the tissue. The cell bodies were surrounded by an empty space, but were not dilacerated. In the dentate gyrus, the dissociation of the cell bodies and of the dendrites from the surrounding neuropil was particularly striking in the control cases (Fig. 3). The neuropil formed a lace-like structure, a "mesh", made of oriented fiber fascicles separated by holes. The fascicles of fibers, making up the mesh, were mainly axonal near the white matter. In the subpial region, the mesh was mostly made of dendritic or astrocytic fibers. Astrocytic feet, isolated by microcryodissection, were observed in contact with capillaries in the Virchow–Robin spaces (Fig. 4). Several years of fixation did not modify the results.

### Senile plaques in the cortex

In the senile plaques, the Aβ positive amyloid core was separated from the neuritic crown after a series of freezing/thawing cycles. CD68 positive phagocytic cells were nearly always seen in contact with the core. Their cytoplasm was demarcated from the neuritic crown and often contained Aβ immunoreactive material. The cytoplasmic location of some Aβ aggregates could be better ascertained on the isolated macrophage separated from its surrounding by the dissection than in the unprocessed tissue. Some of that material was Congo red positive. The phospho-tau positive processes of the crown included thin neurites, devoid of spines, projecting to the core where they ended as dilated boutons that were labeled with anti-NF and anti-synaptophysin antibodies. The pathway followed by the tau positive axons from the periphery to the synaptic contact with the amyloid core could be uniquely identified after the microdissection. Astrocytic processes wrapped the core of the senile plaques. The direct contact of the glial processes with the amyloid core was beautifully illustrated in the microcryodissected plaque, while it was obscured by the neuritic crown in the unprocessed tissue (Fig. 5; supplementary Fig. S3).

### Electron microscopy

Without cryodissection, the core of the senile plaque, the macrophages, the neuritic crown, the macrophages and the glial processes were imbricated. At 80 cycles, a space between the amyloid core and the dystrophic neurites could be observed. The aspect of the plaque constituents was preserved. At 300 freezing/thawing cycles, senile plaques could be seen neither in semi-thin sections nor at the ultrastructural level. The senile plaque probably detached from the section. When the section is too thin, the tissue probably loses its cohesion as a consequence of the large proportion of empty spaces. Of note, the content of the perikaryon of isolated neurons could still be seen with some details. The vessels were also clearly separated from the adjacent neuropil (supplementary Fig. S4).

### Diffuse Aβ deposits in the striatum

Aβ deposits were almost only of the diffuse type in the putamen. Microcryodissection did not dissociate the diffuse deposits themselves but the tissue in which they had developed: the elements of the striatum were separated in the same way whether or not diffuse Aβ deposits

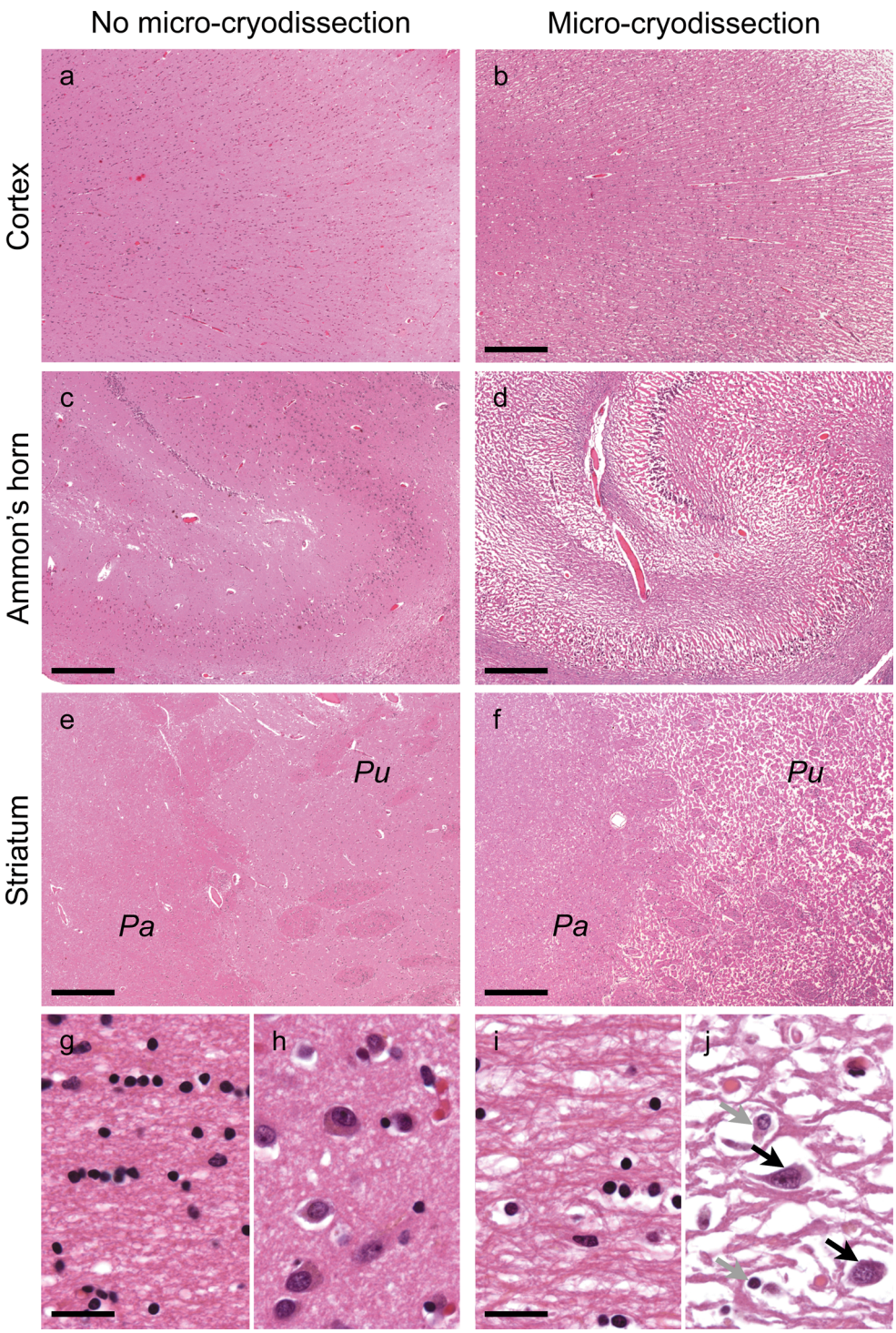


**Fig. 3** Effects of microcryodissection at 300 freezing/thawing cycles. Human brain. Haematoxylin–eosin stain. Sections of neocortex (**a**, **b**), Ammon's horn (**c**, **d**) and striatum (**e**, **f**) without (*left column*) or with (*right column*) microcryodissection. *Pa pallidum*, *Pu putamen*. Aspect of the white matter (**g**, **i**) and grey matter (**h**, **j**) in the neocortex, without (*left column*) or with (*right column*) microcryodissection. The grey matter was better dissociated than the white matter: some cells were completely separated from the adjoining neuropil and were easily identified and analyzed (*black arrows* neurons, *grey arrows* glial cells). **a**–**f** *scale bar* 400 μm, **g**–**j** *scale bar* 20 μm

were present. Neuronal and glial cells were only exceptionally observed around or within the diffuse deposits; Aβ immunoreactivity was never found in their cytoplasm. The smallest deposits of Aβ were granular, ovoid in shape and located in the mesh, most often at a distance of any cell body (supplementary Fig. S5).

## Tau pathology

In areas where neuropil threads were abundant, and specifically in the crown of the senile plaque, the tau positive neurites were fragmented, and dot-like. Continuous fibers were rarer than in tissues that had not been

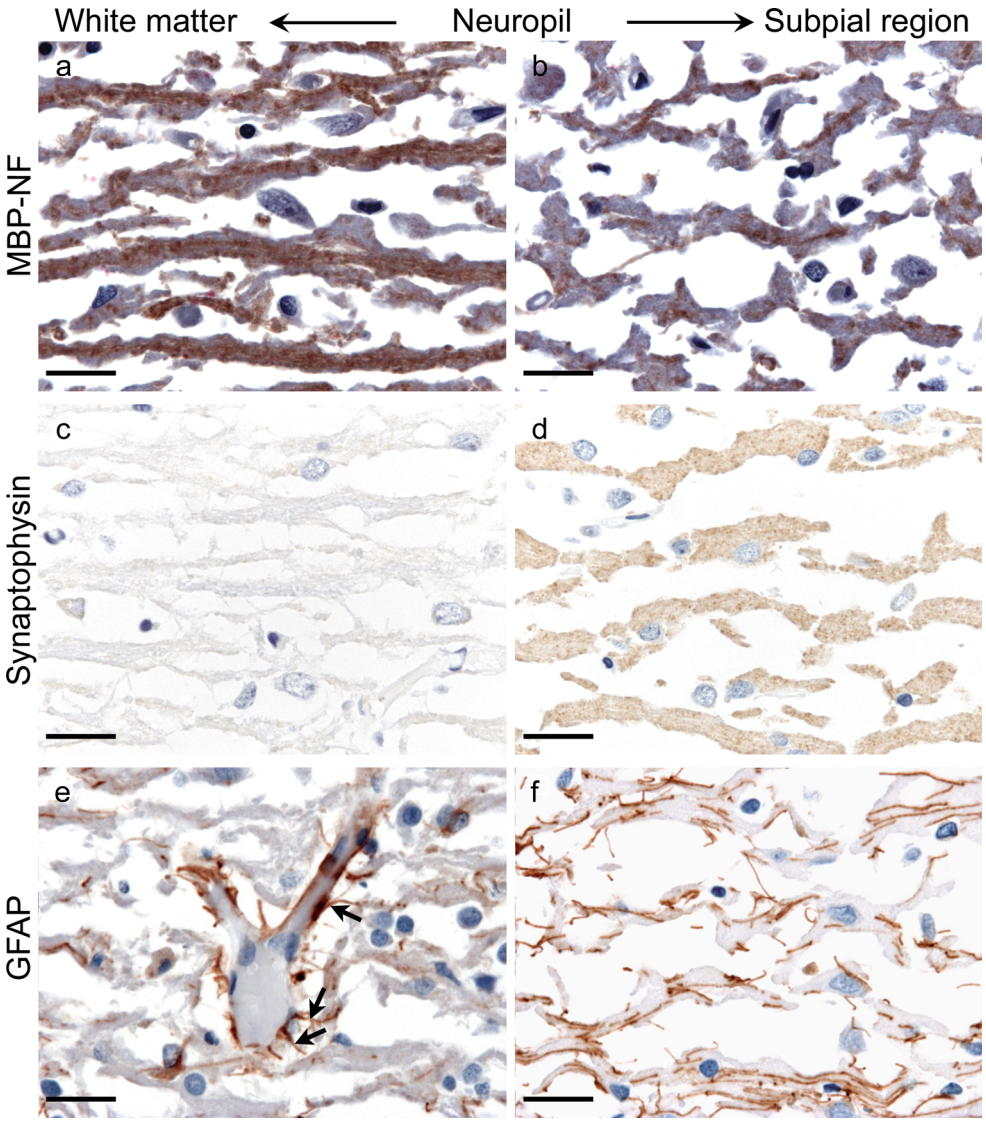


**Fig. 4** Characterization of the lace-like structure obtained by microcryodissection. **a**–**f** Double immunolabelling against myelin basic protein (MBP)/neurofilament (NF). MBP is labeled in *brown* (precipitated DAB) and NF in *red* (Fast Red) (**a**, **b**), anti-synaptophysin (**c**, **d**) and anti-GFAP (**e**, **f**) in the neuropil near the white matter (**a**, **c**, **e**) or in the subpial region (**b**, **d**, **f**) after microcryodissection. In the neuropil near the white matter, the mesh was mostly made of axons (**a**, **c**, **e**). Some astrocytic feet (*arrows*) were observed in contact with isolated vessels. In the neuropil near the subpial region, the mesh was mainly composed of dendrites and astrocytic processes (**b**, **d**, **f**). Human cerebral cortex, *scale bar* 20 μm

cryodissected. Similar aspects of fragmented processes were observed after NF immunohistochemistry. By contrast, some ubiquitin-positive fibers remained continuous. Tau positive fibers or dots resembling synapses were seen in direct contact with the unlabeled cell body of some neurons or, in other instances, with the amyloid core of the plaque itself. A few tau positive dots could also be seen within the core (supplementary Fig. S6).

## Discussion and conclusions

The original technique that we developed—microcryodissection—made use of the dilation of freezing water to dissociate the tissue. The grey matter dissociated into a network of fiber fascicles, alternating with empty spaces in which the cell bodies could usually be found. The proportion of area occupied by those empty spaces increased as the log of the number of cycles. According to Delesse principle (Weibel 1979), the proportion of area on a section is equal to the proportion of volume in three dimensions: the logarithmic relationship remains true for the volume. Surprisingly, the total volume of the microcryodissected samples remained unchanged. The formalin fixation, which induces the development of covalent bonds within the tissue, may act as a limiting factor to the expansion forces. The foci of synchronous expansion, constituted by extracellular empty spaces, may also counteract each other and prevent a general increase of the sample volume. The absence of general expansion and the synchronous dilation of empty spaces may explain why dissociated fibers tended to aggregate into fascicles that appeared wider with the increase in the number of cycles. The fiber dissociation was the finest at 80 cycles. With the increase in the volume of empty spaces, the neuritic and glial processes aggregated in large fascicles that finally formed a mesh. The mesh did not

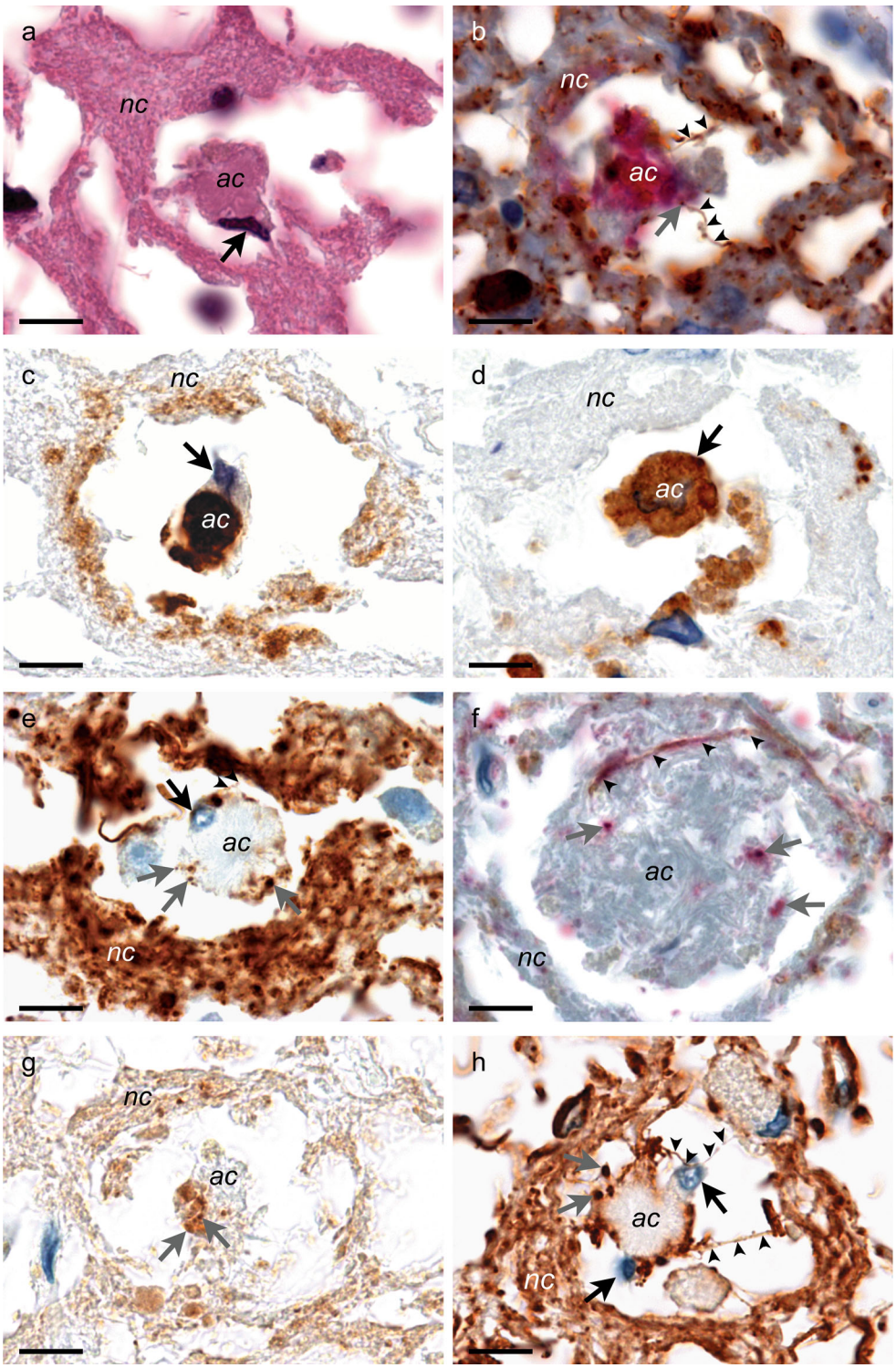
a
nc
ac
b
nc
ac
c
nc
ac
d
nc
ac
e
ac
nc
f
ac
nc
g
nc
ac
h
ac
nc

◀**Fig. 5** Microcryodissection of the senile plaque in the cortex. **a**–**h** Senile plaque. All the pictures were obtained after microcryodissection. Cortex, human brain, *scale bar* 8 μm. **a** Haematoxylin/eosin stain. The neuritic crown ("*nc*" area) surrounded the amyloid core ("*ac*" area), associated with a macrophage (*arrow*). Those elements were dissociated by microcryodissection: the nucleus of the macrophage was stuck to the amyloid core while the crown had been detached from it. **b** Double immunostaining of phospho-tau (AT8) in *brown* and Aβ (6F3D) in *red*. The *arrow heads* point to tau-positive neurites oriented toward the amyloid core. **c** Aβ immunohistochemistry (6F3D). Here again, the macrophage was attached to the amyloid core. The *black arrow* points to its nucleus. Its cell body was filled with Aβ immunoreactive material. **d** CD68 immunohistochemistry. The cytoplasm of the macrophages (*black arrow*) was labeled. Unexpectedly, the core of the senile plaque, separated from the neuropil was also positive. **e** Phospho-tau immunohistochemistry (AT8). The neuritic crown, made of numerous immunoreactive neuropil threads, surrounded the amyloid core. Some thin AT8 positive neurites devoid of any spine (*arrowheads*) were sometimes oriented to the core, where immunoreactive synapse-like *dots* were observed (*grey arrows*). The nucleus of a macrophage is seen attached to the core (*black arrow*). **f** Double labeling myelin basic protein (MBP) in *brown* and neurofilament (NF) in *red*. A naked axon (devoid of MBP) curved around the amyloid core (*arrow heads*); several NF positive profiles are seen within the core (*grey arrows*). **g** Anti-synaptophysin immunohistochemistry: the whole plaque was diffusely labeled. Immunoreactive *dots* were seen in the crown, as well as in contact with the amyloid core (*grey arrows*). **h** GFAP immunohistochemistry. The plaque was wrapped in GFAP positive fibers. Some fibers were oriented toward the core (*arrowheads*). Macrophages were associated to the amyloid core (*black arrows*)

form at random, but followed the orientation of the axons and dendrites present in the neuropil. The pattern of the mesh also depended on the cytoarchitecture. The integrity of the dissociated neuronal, glial and endothelial cells was preserved, at least at the light microscopy level, likely because the cytosolic concentration of diluted solutes prevented freezing at the temperatures reached by the Peltier module (−10/−15 °C). In comparison with the results observed in the grey matter, the dissociation of the white matter was limited (the increase in the volume of empty spaces was nearly six times smaller). A smaller volume of interstitial water in the highly hydrophobic white matter may explain that observation.

Microcryodissection of the senile plaque dissociated the Aβ positive amyloid core from the phospho-tau positive neuritic crown at around 300 cycles. The microglial cells, the axonal processes and the astrocytic wrapping were clearly demarcated. The Aβ positive amyloid core was nearly always associated with active phagocytic cells, the cytoplasm of which sometimes contained Aβ, in some cases Congo red positive. Microcryodissection showed distinctly the adhesion of the microglial cell to the amyloid core by separating the elements of the plaques and improved the resolution of the observation in that respect. It has been suggested that microglia are responsible for the maturation of an initially diffuse deposit into an amyloid core through a process involving endocytosis (Frackowiak et al. 1992). The phospho-tau positive neuritic crown, mainly composed of axons (Schmidt et al. 1991), seemed to project to the center of the plaque, where dystrophic axons ended and several large synapses were observed. The presence of synapses in the neuritic crown was already mentioned in one of the first ultrastructural descriptions of the senile plaque (Gonatas et al. 1967), but their role in its development is not known. Astrocytic processes were also present within the neuritic crown. The presence of a few axonal or astrocytic fibers reaching the core after having crossed the empty space surrounding it could have been considered as a random consequence of the microdissection. The regularity of that observation suggests that it uncovers an intrinsic property of the plaque. Altogether, microcryodissection could help uncover the dynamic interactions between the neuritic crown and the amyloid core.

It has been suggested that extracellular Aβ was produced by neuronal secretion, but diffuse deposits were usually found at a distance from any cell body, making the somatic secretion of Aβ unlikely. More probably, Aβ is directly secreted by the axonal ending (Braak and Del Tredici 2014) although the role of dendritic processes cannot be currently dismissed in some locations (Eisele and Duyckaerts 2016). The orientation of NF and GFAP positive fibers toward and within the amyloid core suggests the attraction of some axons and astrocytic processes by still unknown elements present in the core, maybe produced by microglia.

Several methods of microscopic dissection have been developed with goals that differ from those pursued by microcryodissection. Laser microdissection is performed to extract selected elements in the tissue to proceed to their biochemical analysis, e.g. mass spectrometry or PCR. Selective cellular immunoprecipitation requires the dissociation of the tissue to isolate its constituent cells. Microcryodissection does not extract microsamples or cells from the slide or from the sample but aims at tearing apart the elements of the tissue to facilitate their morphological analysis in situ (e.g. understand the way they are bound together or associated in specific structures such as the senile plaque). Microcryodissection improves the spatial resolution of the microscopic analysis in an unusual but simple way by directly acting on the sample.

**Acknowledgements** Electron microscopy was performed at the imaging platform of Pitié-Salpêtrière (PICPS) located at ICM. Alice Lebois helped to develop the freezing/thawing device. The samples were obtained from the Brain Bank Neuro-CEB (BRIF number 0033-00011), funded by the patients' associations France Parkinson, ARSEP, and "Connaître les Syndromes Cérébelleux" and by LECMA Vaincre Alzheimer, to which we express our gratitude. The

Brain Bank is hosted by the Biological Resource Platform of Pitié-Salpêtrière Hospital, APHP.

## References

Braak H, Braak E (1991) Neuropathological stageing of Alzheimer-related changes. Acta Neuropathol 82:239–259

Braak H, Del Tredici K (2014) Are cases with tau pathology occurring in the absence of Aβ deposits part of the AD-related pathological process? Acta Neuropathol 128:767–772. doi:10.1007/s00401-014-1356-1

Duyckaerts C, Delatour B, Potier M-C (2009) Classification and basic pathology of Alzheimer disease. Acta Neuropathol 118:5–36. doi:10.1007/s00401-009-0532-1

Eisele YS, Duyckaerts C (2016) Propagation of Aβ pathology: hypotheses, discoveries, and yet unresolved questions from experimental and human brain studies. Acta Neuropathol 131:5–25. doi:10.1007/s00401-015-1516-y

Frackowiak J, Wisniewski HM, Wegiel J et al (1992) Ultrastructure of the microglia that phagocytes amyloid and the microglia that produces beta-amyloid fibrils. Acta Neuropathol 84:223–225

Gonatas NK, Anderson W, Evangelista I (1967) The contribution of altered synapses in the senile plaque: an electron microscopic study in Alzheimer's dementia. J Neuropathol Exp Neurol 26:25–39

Ludwig E, Klingler J (1956) Atlas cerebri humani. S. Karger, Basel

Schmidt ML, Lee VM, Trojanowski JQ (1991) Comparative epitope analysis of neuronal cytoskeletal proteins in Alzheimer's disease senile plaque, neurites and neuropil threads. Lab Invest 64:352–357

Thal DR, Rüb U, Orantes M, Braak H (2002) Phases of A beta-deposition in the human brain and its relevance for the development of AD. Neurology 58:1791–1800

Weibel ER (1979) Stereological methods. Practical methods for biological morphometry. Academic Press, London